Review article

Advances in SPECT for Optimizing the Liver Tumors Radioembolization Using Yttrium-90 Microspheres

Hoda Rezaei Roshan, Ahmadreza Azarm, Babak Mahmoudian[1], Jalil Pirayesh Islamian

Departments of Medical Physics and [1]Radiology, Nuclear Medicine Unit, Faculty of Medicine, Tabriz University of Medical Sciences, Tabriz, Iran

Abstract

Radioembolization (RE) with Yttrium-90 (^{90}Y) microspheres is an effective treatment for unresectable liver tumors. The activity of the microspheres to be administered should be calculated based on the type of microspheres. Technetium-99m macroaggregated albumin (^{99m}Tc-MAA) single photon emission computed tomography/computed tomography (SPECT/CT) is a reliable assessment before RE to ensure the safe delivery of microspheres into the target. ^{90}Y bremsstrahlung SPECT imaging as a posttherapeutic assessment approach enables the reliable determination of absorbed dose, which is indispensable for the verification of treatment efficacy. This article intends to provide a review of the methods of optimizing ^{90}Y bremsstrahlung SPECT imaging to improve the treatment efficacy of liver tumor RE using ^{90}Y microspheres.

Keywords: Bremsstrahlung SPECT, radioembolization, single photon emission computed tomography/computed tomography, Yttrium-90 microspheres

Introduction

Radioembolization (RE) with Yttrium-90 (^{90}Y) microspheres by hepatic arterial administration is the effective treatment for unresectable primary and metastatic liver cancers.[1,2] Transarterial chemoembolization (TACE) is a conventional treatment for unresectable hepatocellular carcinoma (HCC).[3] The therapeutic benefit of the hepatic arterial approach is based on the unique dual vascular supply of the liver.[4,5] It should also be noted that postembolization syndrome following RE with ^{90}Y microspheres is less intense than after TACE, as RE has a longer time to progression and less toxicity than chemoembolization.[6,7] Selective internal radiotherapy (SIRT) with ^{90}Y microspheres has been increasingly used over the past decade for RE of inoperable liver metastases of colorectal cancer (CRC), although its first clinical trials date back to the early 1960s.[8] The physiological basis for tumor targeting in SIRT is an increased arterial vascularization of the targeted tumor compared to the normal liver parenchyma.[9,10] In addition, ^{90}Y-labeled monoclonal antibodies such as ^{90}Y Zevalin (ibritumomab tiuxetan) can be used in targeted radionuclide therapy (TRT) for the radioimmunotherapy of malignant diseases such as non-Hodgkin lymphoma.[11-13] Unresectable liver cancer causes a lot of suffering worldwide and eventual death in many patients.[14] RE involves the infusion of ^{90}Y microspheres into the hepatic arterial circulation, from which approximately 80-100% liver tumor blood flow is derived.[15] ^{90}Y RE is an effective treatment of HCC if the ^{90}Y microspheres accumulate in the right location, at the right dose, and with the right intent.[16,17]

Inadvertent delivery of ^{90}Y microspheres into the hepatic arteries and subsequently nontarget localization—and thus offtarget irradiation—can lead to some severe complications after RE, such as acute radiation dermatitis of the abdominal wall, periumbilical and abdominal pain, gastrointestinal ulceration/bleeding, cholecystitis, pancreatitis, radiation pneumonitis, and hepatic decompensation.[18-20] As the hepatic vascular anatomy and tumor-to-normal arterial blood flow ratio are highly variable between metastases and between different patients, it is essential to plan and perform, before RE with ^{90}Y microspheres, specific treatment simulation

Access this article online

Quick Response Code:

Website: www.wjnm.org

DOI: 10.4103/1450-1147.157120

Address for correspondence:
Dr. Jalil Pirayesh Islamian, Department of Medical Physics, School of Medicine, Tabriz University of Medical Sciences, Attar Neyshapouri Street, Azadi Avenue, Tabriz - 5166614766, Iran. E-mail: pirayeshj@gmail.com

before the real therapy to rule out any side effects.[21,22] Technetium-99m macroaggregated albumin (^{99m}Tc-MAA) scintigraphy by single photon emission computed tomography (SPECT) in combination with computed tomography (CT), that is, SPECT/CT should be recommended in a pretherapeutic assessment in order to establish dependable treatment planning, metabolic response, and a predictive dosimetric model.[23,24] In addition, tumor-to-normal activity concentration ratio and the biodistribution of ^{90}Y microspheres are two crucial parameters for confirming the effectiveness of RE with ^{90}Y microspheres.[25,26] Posttherapeutic assessment is indispensable in evaluating the abovementioned physical and physiological parameters. Posttherapy dosimetry on the basis of the ^{90}Y bremsstrahlung SPECT imaging is a useful tool to verify absorbed dose delivery.[27] The role of SPECT in diagnostic imaging and internal dosimetry is well established in nuclear medicine.[28] A considerable amount of literature has been published on RE with ^{90}Y resin or glass microspheres as an effective treatment of unresectable liver tumors or metastases, whereas there has been relatively scarce literature focused on the role of SPECT as a complementary method to this therapeutic treatment. In the present review, the role of SPECT imaging as the posttherapeutic and pretherapeutic assessment modality is evaluated for RE using ^{90}Y microspheres. Moreover, we discussed the recently-used optimization approach for quantitative ^{90}Y bremsstrahlung SPECT imaging.

^{90}Y Microspheres and Activity Determination

^{90}Y is a pure beta-emitting isotope with a physical half-life of 2.67 days. The emitted particles have a maximum energy of 2.27 MeV, a mean energy of 0.93 MeV, and an average penetration range of 2.5 mm, with a maximum 11 mm range in tissue. The ^{90}Y can be labeled with resin or glass microspheres that have been approved by the Food and Drug Administration (FDA).[29,30] Both glass microspheres (TheraSphere, MDS Nordion, Ottawa, Ontario, Canada) and resin microspheres (SIR-Spheres, Sirtex Medical, Sydney, Australia) are used to treat hepatic primary and metastatic neoplasms.[31] In spite of the many similarities, there are some differences between the two types from the point of view of dosimetry and performance. The resin type is used adjuvant to chemotherapy with floxuridine, as well, with fluorouracil (5-FU) as the radiosensitizing agent.[10,29] Microsphere reflux during administration is the main cause of gastroduodenal ulcer.[32] The risk of reflux in the case of resin microspheres is greater than in glass due to an embolic tendency of resin related to its lower specific activity and the subsequent higher number of microspheres required with the same activity compared to the glass type.[33] The characteristics of both types of microspheres are shown in Table 1.

Table 1: Characteristics of the glass and resin ^{90}Y microsphere agents

Characteristic	Glass microsphere (TheraSphere)	Resin microsphere (SIR-Spheres)
Specific activity (Bq per sphere)	2500	50
Dose to tumor volume	No	Yes
Adjuvant to chemotherapy	No	Yes
Mean number of spheres per dose (×10^6)	4	50
Median diameter (μm)	25	35

Based on the assumptions that ^{90}Y glass microspheres are uniformly distributed in the liver volume and with a nominal average target dose of 150 Gy/kg, the required activity of the glass microspheres in RE could be calculated by Equation 1:

$$A_{glass}(\mathrm{GBq}) = \frac{\mathrm{D(Gy)} \times \mathrm{M(kg)}}{50(\frac{\mathrm{Gy.kg}}{\mathrm{GBq}})} \quad \text{Equation 1}$$

where A_{glass} is the activity of the ^{90}Y glass microspheres, D is the nominal target dose, and M is the liver mass that was calculated from the CT data. Currently, the activity of the resin microspheres in RE is determined by the following three methods, based on the assumption that ^{90}Y resin microspheres are nonuniformly distributed in the liver tumor volume:.[34,35]

The body surface area method

This method is the most common/widely used method to calculate activity for ^{90}Y resin microspheres. The BSA is calculated by Equation 2:[36]

$$\mathrm{BSA} = 0.20247 \times h(m)^{0.725} \times w(kg)^{0.425} \quad \text{Equation 2}$$

where h and w are the patient's height and weight, respectively. The required activity of the ^{90}Y resin microspheres was calculated by Equation 3:

$$\mathrm{A_{resin}(GBq)} = (\mathrm{BSA} - 0.2) + (\frac{V_{tumor}}{V_{tumor} + V_{liver}}) \quad \text{Equation 3}$$

where $\mathrm{A_{resin}}$ is the activity of the ^{90}Y resin microspheres and and the volumes of the tumor and liver, respectively.[29]

The empirical method

The usability of the empirical method is related to the accuracy of CT or magnetic resonance imaging (MRI) in the differentiation of the degree of liver involvement by the tumor. According to this method, administration of 2.0 GBq for <25% involvement, 2.5 GBq for 25-50% involvement, and 3.0 GBq for >50% involvement is appropriate in liver tumor RE. One of the deficiencies of this method is its low safety margin.[37]

Partition model method

The calculation of ^{90}Y resin microsphere activity by using the partition model method is based on the information

obtained from ^{99m}Tc-MAA planar or SPECT/CT imaging.[38] This model is usually applicable for discrete and solitary hepatic tumors. The activity calculated by this method is higher than that suggested by the empirical and BSA methods, with an equivalent safety threshold.[35]

SPECT in Pretherapeutic Assessment

^{99m}Tc-MAA scintigraphy should be performed before liver tumor RE and also prior to the activity calculation using ^{90}Y to arrive at the accurate treatment plan and to estimate the tumor-to-normal activity ratio, as well as minimizing the radiation risk to the normal parenchymas in view of the fact that normal parenchymas have a lower tolerance for the treatment dose.[39,40] The particle size and biodistribution of ^{99m}Tc-MAA is similar to the ^{90}Y resin microspheres [Figure 1].[3] ^{99m}Tc-MAA SPECT imaging done before RE is superior to planar imaging with regard to the detection of gall bladder uptake and extrahepatic shunting to the gastrointestinal or pulmonary tract. Furthermore, SPECT combined with integrated low-dose CT increases sensitivity and specificity, and thus the detection accuracy of extrahepatic radiotracer activity, and this in turn decreases the toxicity and incidence of complications in RE.[10,28] The spatial resolution and image quality of SPECT imaging are strongly depend on the type of collimator, reconstruction algorithm, and acquisition energy window. Therefore, a low-energy high-resolution (LEHR) parallel-hole collimator and iterative reconstruction algorithms such as ordered subset expectation maximization (OSEM) with a 10% or 20% energy window centered at the peak of ^{99m}Tc (140 keV) are preferred for ^{99m}Tc-MAA SPECT imaging.[41,42]

SPECT in posttherapeutic assessment

The treatment efficacy of RE, according to the ^{90}Y biodistribution image and quantitative assessment of the tumor-to-normal dose ratio, is a reliable parameter for the treatment.[43] ^{90}Y bremsstrahlung SPECT imaging after RE has shown great potential to provide a reliable dose evaluation, which is essential for dose verification; additionally, CT in combination with ^{90}Y bremsstrahlung SPECT is used for attenuation and scatter correction, and this further increases quantitative accuracy.[4,44] Quantitatively, ^{90}Y bremsstrahlung SPECT imaging is one of the most challenging topics in nuclear medicine. Here, too, the image quality and quantification accuracy of the ^{90}Y bremsstrahlung SPECT imaging strongly depend on the type of collimator, reconstruction algorithm, and acquisition energy window.[45]

Energy window optimizing for ^{90}Y bremsstrahlung SPECT

In conventional nuclear medicine imaging, gamma-emitter radioisotopes with a pronounced photopeak, such as ^{99m}Tc, are used for imaging, and the acquisition energy window placed around the photopeak. In contrast, ^{90}Y bremsstrahlung photons arise from the interaction of β-particles with the patient body and have a continuous and broad energy spectrum extending up to the highest beta energy emission (2.3 MeV) without a pronounced photopeak.[46] Therefore, the choice of the acquisition energy window strongly affects the reliability of the dose and the activity estimation. Figure 2 shows a typical ^{90}Y bremsstrahlung energy spectrum. In ^{90}Y imaging, only the primary photons are suitable, but the scatter-to-primary ratio is significant in any energy window.[43,47] The main problem in ^{90}Y imaging is that the photons with energies less than 60 keV have attenuated

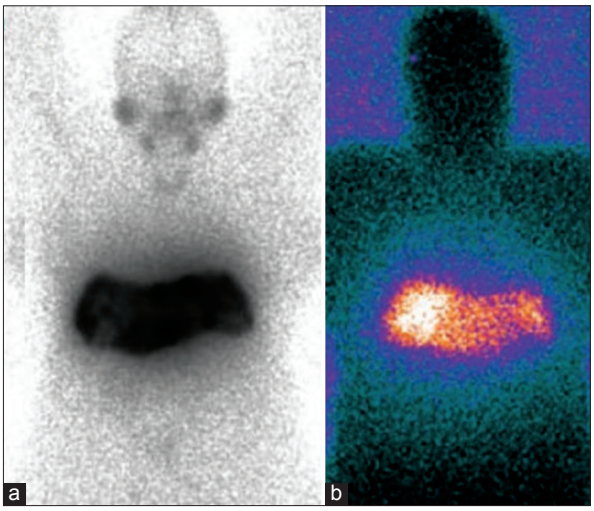

Figure 1: A typical gamma camera scan (a) after accumulated 99mTc-MAA within the liver with no extrahepatic shunting and (b) bremsstrahlung scan within 1 h after 90Y microspheres were administered intra-arterially in the same patient

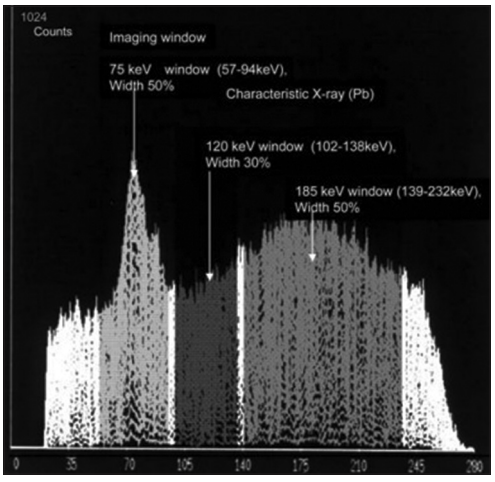

Figure 2: A typical 90Y bremsstrahlung energy spectrum was obtained using a gamma camera equipped with a MEGP collimator. Three energy window widths of 50% (57-94 keV) centered at 75 keV, 30% (102-138 keV) at 120 keV, and 50% (139-232 keV) at 185 keV were set on the spectrum

in the patient body and those with energies higher than 500 keV have penetrated through or been scattered by the collimator septa; however, the optimal acquisition energy window is in the energy range. On the other hand, the highest percentage of photons with the energy range 160-300 keV arise from the backscattered compartment behind the crystal, and those with the energy range 300-2000 keV arise from penetration through or scattering by the collimator septa. A characteristic x-ray peak appeared at 75 keV due to the interaction between the bremsstrahlung photons and lead (Pb) in the collimator decreasing the signal-to-noise ratio (SNR). These photons degrade image quality and quantitative accuracy.[48,49] The dominant effect with a narrow energy window is noise, owing to the low count level and low system sensitivity, as an undesirable effect. On the other hand, for a wide energy window the most critical image-degrading factor is beam-hardening artifacts. It is agreed that the 100-160 keV is the optimal energy window, as this range has a lower scatter-to-primary ratio and therefore ensures the highest accuracy in dose determination.[50,51] As a whole, both the single-energy window (SEW) and multiple-energy window (MEW) methods are used to choose the optimal energy window for ^{90}Y bremsstrahlung SPECT imaging. Shigeki Ito *et al*. have shown, on the basis of the multiple-energy range (MER) method, that three energy peaks centered around 75 keV (50%), 120 keV (30%), and 18 5 keV (50%) provide the highest system sensitivity and the lowest imaging acquisition time suitable for clinical imaging. In addition, it should be noted that there is a trade-off relationship between sensitivity and spatial resolution, so it is expected that the more the sensitivity, the less the image quality.[43]

Collimator and reconstruction algorithm optimizing for ^{90}Y bremsstrahlung SPECT

The OSEM iterative reconstruction algorithm optimizes the quantitative accuracy of ^{90}Y bremsstrahlung SPECT and eliminates streak artifact, compared with the conventional filtered backprojection (FBP) reconstruction algorithm.[21] The collimator in SPECT is a critical component of the imaging chain and has a major impact on activity estimation. Routinely, ^{90}Y bremsstrahlung SPECT imaging is performed with a high-energy general-purpose (HEGP) collimator or with a medium-energy general-purpose (MEGP) parallel-hole collimator, which is designed for high-energy isotopes such as gallium-67 (^{67}Ga) and iodine-131 (^{131}I), and yet a special parallel-hole collimator has never been fabricated for ^{90}Y bremsstrahlung SPECT imaging [Figure 3].[52] Rotating slat collimators and pinhole collimators have been proposed for SPECT imaging with high-energy isotopes and isotopes with extensive energy spectra.[45,53,54] Xing Rong *et al*. have proposed an optimal parallel-hole collimator with a small amount of septal scatter and penetration for quantitative ^{90}Y bremsstrahlung SPECT imaging.[55]

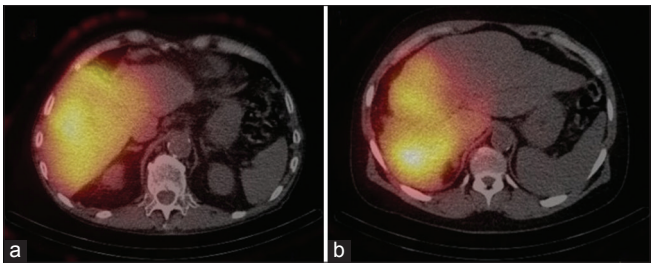

Figure 3: Typical bremsstrahlung SPECT scans after RE with 90Y microspheres were acquired with (a) a MEGP collimator and (b) a HEGP collimator. Energy window was set for 100-150 keV

Conclusion

RE with ^{90}Y is an effective treatment for hepatic tumors. The quantity of the administered activity for ^{90}Y resin or glass microspheres is an influential parameter in the effectiveness of the RE. The required activity of the ^{90}Y microspheres is determined based on the type of microspheres. ^{99m}Tc-MAA SPECT/CT before RE constitutes appropriate pretherapy planning and enables predictive dosimetry, thus presenting as a valuable diagnostic tool regarding the biodistribution of ^{90}Y microspheres. ^{90}Y bremsstrahlung SPECT imaging after RE should be used to verify the therapy's clinical effectiveness and to obtain a precise absorbed dose delivery pattern. Finally, the collimator, reconstruction algorithm, and acquisition energy window are important components in ^{90}Y bremsstrahlung SPECT imaging and play key roles in image quality, quantitative accuracy, and accurate dosimetry. Therefore, the optimization of these parameters leads to improved treatment efficacy and ^{90}Y bremsstrahlung SPECT image quality/quantity.

References

1. Jakobs TF, Hoffmann RT, Poepperl G, Schmitz A, Lutz J, Koch W, *et al*. Mid-term results in otherwise treatment refractory primary or secondary liver confined tumours treated with selective internal radiation therapy (SIRT) using (90) Yttrium resin-microspheres. Eur Radiol 2007;17:1320-30.
2. Geschwind JF, Salem R, Carr BI, Soulen MC, Thurston KG, Goin KA, *et al*. Yttrium-90 microspheres for the treatment of hepatocellular carcinoma. Gastroenterology 2004;127(Suppl 1):S194-205.
3. Peynircioğlu B, Cil B, Bozkurt F, Aydemir E, Uğur O, Balkanci F. Radioembolization for the treatment of unresectable liver cancer: Initial experience at a single center. Diagn Interv Radiol 2010;16:70-8.
4. Sato K, Lewandowski RJ, Bui JT, Omary R, Hunter RD, Kulik L, *et al*. Treatment of unresectable primary and metastatic liver cancer with yttrium-90 microspheres (TheraSphere): Assessment of hepatic arterial embolization. Cardiovasc Intervent Radiol 2006;29:522-9.

5. Gulec SA, Fong Y. Yttrium 90 microsphere selective internal radiation treatment of hepatic colorectal metastases. Arch Surg 2007;142:675-82.
6. Salem R, Thurston KG. Radioembolization with ^{90}yttrium microspheres: A state-of-the-art brachytherapy treatment for primary and secondary liver malignancies: Part 1: Technical and methodologic considerations. J Vasc Interv Radiol 2006;17:1251-78.
7. Salem R, Lewandowski RJ, Kulik L, Wang E, Riaz A, Ryu RK, *et al*. Radioembolization results in longer time-to-progression and reduced toxicity compared with chemoembolization in patients with hepatocellular carcinoma. Gastroenterology 2011;140:497-507. e2.
8. Dawson LA, McGinn CJ, Normolle D, Ten Haken RK, Walker S, Ensminger W, *et al*. Escalated focal liver radiation and concurrent hepatic artery fluorodeoxyuridine for unresectable intrahepatic malignancies. J Clin Oncol 2000;18:2210-8.
9. Tan AE, Kao YH, Xie W. Excessive hepatic arterial-portal venous shunting may predict failure of microparticle localization in hepatocellular carcinomas. World J Nucl Med 2013;12:48-50.
10. Flamen P, Vanderlinden B, Delatte P, Ghanem G, Ameye L, Van Den Eynde M, *et al*. Multimodality imaging can predict the metabolic response of unresectable colorectal liver metastases to radioembolization therapy with Yttrium-90 labeled resin microspheres. Phys Med Biol 2008;53:6591-603.
11. Wiseman GA, White CA, Stabin M, Dunn WL, Erwin W, Dahlbom M, *et al*. Phase I/II 90Y-Zevalin (yttrium-90 ibritumomab tiuxetan, IDEC-Y2B8) radioimmunotherapy dosimetry results in relapsed or refractory non-Hodgkin's lymphoma. Eur J Nucl Med 2000;27:766-77.
12. Gordon LI, Molina A, Witzig T, Emmanouilides C, Raubtischek A, Darif M, *et al*. Durable responses after ibritumomab tiuxetan radioimmunotherapy for CD20+B-cell lymphoma: Long-term follow-up of a phase 1/2 study. Blood 2004;103:4429-31.
13. Otte A. Diagnostic imaging prior to 90Y-ibritumomab tiuxetan (Zevalin) treatment in follicular non-Hodgkin's lymphoma. Hell J Nucl Med 2008;11:12-5.
14. Jemal A, Murray T, Ward E, Samuels A, Tiwari RC, Ghafoor A, *et al*. Cancer statistics, 2005. CA Cancer J Clin 2005;55:10-30.
15. Kennedy AS, Nutting C, Coldwell D, Gaiser J, Drachenberg C. Pathologic response and microdosimetry of (90) Y microspheres in man: Review of four explanted whole livers. Int J Radiat Oncol Biol Phys 2004;60:1552-63.
16. Kao YH, Hock Tan AE, Burgmans MC, Irani FG, Khoo LS, Gong Lo RH, *et al*. Image-guided personalized predictive dosimetry by artery-specific SPECT/CT partition modeling for safe and effective 90Y radioembolization. J Nucl Med 2012;53:559-66.
17. Hilgard P, Hamami M, Fouly AE, Scherag A, Müller S, Ertle J, *et al*. Radioembolization with yttrium-90 glass microspheres in hepatocellular carcinoma: European experience on safety and long-term survival. Hepatology 2010;52:1741-9.
18. Riaz A, Lewandowski RJ, Kulik LM, Mulcahy MF, Sato KT, Ryu RK, *et al*. Complications following radioembolization with yttrium-90 microspheres: A comprehensive literature review. J Vasc Interv Radiol 2009;20:1121-31.
19. Leong QM, Lai HK, Lo RG, Teo TK, Goh A, Chow PK. Radiation dermatitis following radioembolization for hepatocellular carcinoma: A case for prophylactic embolization of a patent falciform artery. J Vasc Interv Radiol 2009;20:833-6.
20. Yip D, Allen R, Ashton C, Jain S. Radiation-induced ulceration of the stomach secondary to hepatic embolization with radioactive yttrium microspheres in the treatment of metastatic colon cancer. J Gastroenterol Hepatol 2004;19:347-9.
21. Ahmadzadehfar H, Muckle M, Sabet A, Wilhelm K, Kuhl C, Biermann K, *et al*. The significance of bremsstrahlung SPECT/CT after yttrium-90 radioembolization treatment in the prediction of extrahepatic side effects. Eur J Nucl Med Mol Imaging 2011. [Epub ahead of print]
22. Denecke T, Rühl R, Hildebrandt B, Stelter L, Grieser C, Stiepani H, *et al*. Planning transarterial radioembolization of colorectal liver metastases with Yttrium 90 microspheres: Evaluation of a sequential diagnostic approach using radiologic and nuclear medicine imaging techniques. Eur Radiol 2008;18:892-902.
23. Sgouros G, Frey E, Wahl R, He B, Prideaux A, Hobbs R. Three-dimensional imaging-based radiobiological dosimetry. Semin Nucl Med 2008;38:321-34.
24. Lenoir L, Edeline J, Rolland Y, Pracht M, Raoul JL, Ardisson V, *et al*. Usefulness and pitfalls of MAA SPECT/CT in identifying digestive extrahepatic uptake when planning liver radioembolization. Eur J Nucl Med Mol Imaging 2012;39:872-80.
25. Ahmadzadehfar H, Duan H, Haug AR, Walrand S, Hoffmann M. The role of SPECT/CT in radioembolization of liver tumours. Eur J Nucl Med Mol Imaging 2014;41(Suppl 1):S115-24.
26. Fabbri C, Sarti G, Cremonesi M, Ferrari M, Di Dia A, Agostini M, *et al*. Quantitative analysis of 90Y Bremsstrahlung SPECT-CT images for application to 3D patient-specific dosimetry. Cancer Biother Radiopharm 2009;24:145-54.
27. Giammarile F, Bodei L, Chiesa C, Flux G, Forrer F, Kraeber-Bodere F, *et al*.; Therapy, Oncology and Dosimetry Committees. EANM procedure guideline for the treatment of liver cancer and liver metastases with intra-arterial radioactive compounds. Eur J Nucl Med Mol Imaging 2011;38:1393-406.
28. Hamami ME, Poeppel TD, Müller S, Heusner T, Bockisch A, Hilgard P, *et al*. SPECT/CT with 99mTc-MAA in radioembolization with 90Y microspheres in patients with hepatocellular cancer. J Nucl Med 2009;50:688-92.
29. Murthy R, Nunez R, Szklaruk J, Erwin W, Madoff DC, Gupta S, *et al*. Yttrium-90 microsphere therapy for hepatic malignancy: Devices, indications, technical considerations, and potential complications. Radiographics 2005;25(Suppl 1):S41-55.
30. Ahmadzadehfar H, Biersack HJ, Ezziddin S. Radioembolization of liver tumors with yttrium-90 microspheres. Semin Nucl Med 2010;40:105-21.
31. Salem R, Lewandowski R, Roberts C, Goin J, Thurston K, Abouljoud M, *et al*. Use of Yttrium-90 glass microspheres (TheraSphere) for the treatment of unresectable hepatocellular carcinoma in patients with portal vein thrombosis. J Vasc Interv Radiol 2004;15:335-45.
32. Naymagon S, Warner RR, Patel K, Harpaz N, Machac J, Weintraub JL, *et al*. Gastroduodenal ulceration associated with radioembolization for the treatment of hepatic tumors: An institutional experience and review of the literature. Dig Dis Sci 2010;55:2450-8.
33. Konda A, Savin MA, Cappell MS, Duffy MC. Radiation microsphere-induced GI ulcers after selective internal radiation therapy for hepatic tumors: An underrecognized clinical entity. Gastrointest Endosc 2009;70:561-7.
34. Murthy R, Kamat P, Nuñez R, Salem R. Radioembolization of yttrium-90 microspheres for hepatic malignancy. Semin Intervent Radiol 2008;25:48-57.
35. Lau WY, Kennedy AS, Kim YH, Lai HK, Lee RC, Leung TW, *et al*. Patient selection and activity planning guide for selective internal radiotherapy with yttrium-90 resin microspheres. Int J Radiat Oncol Biol Phys 2012;82:401-7.
36. Du Bois D, Du Bois EF. A formula to estimate the approximate surface area if height and weight be known. 1916. Nutrition 1989;5:303-13.
37. Kennedy AS, McNeillie P, Dezarn WA, Nutting C, Sangro B, Wertman D, *et al*. Treatment parameters and outcome in 680 treatments of internal radiation with resin 90Y-microspheres

for unresectable hepatic tumors. Int J Radiat Oncol Biol Phys 2009;74:1494-500.

38. Sarfaraz M, Kennedy AS, Lodge MA, Li XA, Wu X, Yu CX. Radiation absorbed dose distribution in a patient treated with yttrium-90 microspheres for hepatocellular carcinoma. Med Phys 2004;31:2449-53.
39. Gray BN, Burton MA, Kelleher D, Klemp P, Matz L. Tolerance of the liver to the effects of Yttrium-90 radiation. Int J Radiat Oncol Biol Phys 1990;18:619-23.
40. Garin E, Rolland Y, Lenoir L, Pracht M, Mesbah H, Porée P, *et al*. Utility of quantitative Tc-MAA SPECT/CT for yttrium-labelled microsphere treatment planning: Calculating vascularized hepatic volume and dosimetric approach. Int J Mol Imaging 2011;2011:398051.
41. Van De Wiele C, Stellamans K, Brugman E, Mees G, De Spiegeleer B, D'Asseler Y, *et al*. Quantitative *P* retreatment VOI analysis of liver metastases. (99m) Tc-MAA SPECT/CT and FDG PET/CT in relation with treatment response to SIRT. Nuklearmedizin 2013;52:21-7.
42. Ahmadzadehfar H, Sabet A, Muckle M, Wilhelm K, Reichmann K, Biersack HJ, *et al*. 99mTc-MAA/90Y-Bremsstrahlung SPECT/CT after simultaneous Tc-MAA/90Y-microsphere injection for immediate treatment monitoring and further therapy planning for radioembolization. Eur J Nucl Med Mol Imaging 2011;38:1281-8.
43. Ito S, Kurosawa H, Kasahara H, Teraoka S, Ariga E, Deji S, *et al*. 90Y bremsstrahlung emission computed tomography using gamma cameras. Ann Nucl Med 2009;23:257-67.
44. Minarik D, Sjögreen Gleisner K, Ljungberg M. Evaluation of quantitative (90) Y SPECT based on experimental phantom studies. Phys Med Biol 2008;53:5689-703.
45. Walrand S, Hesse M, Wojcik R, Lhommel R, Jamar F. Optimal design of anger camera for bremsstrahlung imaging: Monte Carlo evaluation. Front Oncol 2014;4:149.
46. Rong X, Ghaly M, Frey EC. Optimization of energy window for 90Y bremsstrahlung SPECT imaging for detection tasks using the ideal observer with model-mismatch. Med Phys 2013;40:062502.
47. Rong X, Du Y, Ljungberg M, Rault E, Vandenberghe S, Frey EC. Development and evaluation of an improved quantitative (90) Y bremsstrahlung SPECT method. Med Phys 2012;39:2346-58.
48. Shen S, DeNardo GL, Yuan A, DeNardo DA, DeNardo SJ. Planar gamma camera imaging and quantitation of yttrium-90 bremsstrahlung. J Nucl Med 1994;35:1381-9.
49. Walrand S, Flux GD, Konijnenberg MW, Valkema R, Krenning EP, Lhommel R, *et al*. Dosimetry of yttrium-labelled radiopharmaceuticals for internal therapy: 86Y or 90Y imaging? Eur J Nucl Med Mol Imaging 2011;38(Suppl 1):S57-68.
50. Heard S, Flux GD, Guy MJ, Ott RJ. Monte Carlo simulation of ^{90}Y Bremsstrahlung imaging. IEEE Nucl Sci Symp Conf Rec 2004;6:3579-83.
51. Rong X, Du Y, Frey EC. A method for energy window optimization for quantitative tasks that includes the effects of model-mismatch on bias: Application to Y-90 bremsstrahlung SPECT imaging. Phys Med Biol 2012;57:3711-25.
52. Talanow R. Quality analysis of different collimators and energy window aquisitions for Bremsstrahlung SPECT/CT. European Congress of Radiology, 2011.
53. Van Holen R, Staelens S, Vandenberghe S. SPECT imaging of high energy isotopes and isotopes with high energy contaminants with rotating slat collimators. Med Phys 2009;36:4257-67.
54. Walrand S, Hesse M, Demonceau G, Pauwels S, Jamar F. Yttrium-90-labeled microsphere tracking during liver selective internal radiotherapy by bremsstrahlung pinhole SPECT: Feasibility study and evaluation in an abdominal phantom. EJNMMI Res 2011;1:32.
55. Rong X, Frey EC. A collimator optimization method for quantitative imaging: Application to Y-90 bremsstrahlung SPECT. Med Phys 2013;40:082504.

How to cite this article: Roshan HR, Azarm A, Mahmoudian B, Islamian JP. Advances in SPECT for Optimizing the Liver Tumors Radioembolization Using Yttrium-90 Microspheres. World J Nucl Med 2015;14:75-80.

Source of Support: Nil, **Conflict of Interest:** None declared.